



PAPER

Second solar ultraviolet radiometer comparison campaign UVC-II

To cite this article: Gregor Hülsen *et al* 2020 *Metrologia* **57** 035001

View the [article online](#) for updates and enhancements.

Second solar ultraviolet radiometer comparison campaign UVC-II

Gregor Hülsen^{1,11}, Julian Gröbner¹, Alkis Bais² , Mario Blumthaler³, Henri Diémoz⁴, David Bolsée⁵, Ana Diaz⁶, Ilias Fountoulakis⁴, Erik Naranen⁷, Josef Schreder⁸, Facta Stefania⁹ and José Manuel Vilaplana Guerrero¹⁰

¹ Physikalisch-Meteorologisches Observatorium Davos, World Radiation Center (PMOD/WRC), Davos, Switzerland

² Aristotle University of Thessaloniki, Laboratory of Atmospheric Physics (LAP-AUTH), 54124 Thessaloniki, Greece

³ Medizinische Universität Innsbruck, Sektion für Biomedizinische Physik (UIIMP), Müllerstrasse 44, 6020 Innsbruck, Austria

⁴ Agenzia Regionale per la Protezione dell'Ambiente (ARPA) Valle d'Aosta, Loc. La Maladire, Rue de La Maladire, 48, 11020 Saint-Christophe, Italy

⁵ Royal Belgian Institute for Space Aeronomy, BIRA-IASB, 3 Avenue Circulaire, 1180 Brussels, Belgium

⁶ Agencia Estatal de Meteorología (AEMET), Servicio Redes Especiales y Vigilancia Atmosférica, Leonardo Prieto Castro 6, 28071 Madrid, Spain

⁷ ISO-CAL North America, LLC, 36610 N 20th Street, Phoenix, AZ 85086 United States of America

⁸ CMS Ing. Dr Schreder GmbH, Eggerstrasse 8, 6322 Kirchbichl, Austria

⁹ Agenzia Regionale per la Protezione dell'Ambiente (ARPA) Piemonte, Via Jervis 30, 10015 Ivrea, Italy

¹⁰ Instituto Nacional de Técnica Aeroespacial (INTA), Huelva-Matalascañas Road, km.33, 21130 Huelva-Matalascañas Road km.33, Spain

E-mail: gregor.huelsen@pmodwrc.ch

Received 16 December 2019, revised 10 February 2020

Accepted for publication 11 February 2020

Published 6 May 2020



Abstract

In 2017, PMOD/WRC organised the solar ultraviolet broadband radiometer comparison campaign UVC-II. All 75 participating instruments from all over the world were characterised in the laboratory of the World Calibration Center for UV (WCCUV) and calibrated outdoors relative to the QASUME reference spectroradiometer. After a three month calibration period, all devices were returned to their owners, accompanied by a certificate demonstrating traceability to the international system of units. The calibration uncertainty stated in these certificates was less than 6% for the majority of the radiometers. The deviation to the original calibration factors was analysed. From this data we determined three components affecting the overall measurement uncertainty of solar UV measurements using broadband radiometers on different time scales: Usage of additional correction factors to the absolute calibration factor, control of the humidity inside the device and recalibration frequency. A subset of radiometers participating in the campaign were calibrated and characterised at their home laboratories. A comparison of the calibration factors shows that the USER- and the WCCUV-calibrations agree within the uncertainties for 9 out of 11 calibrations.

Keywords: calibration, ultraviolet, solar radiation

(Some figures may appear in colour only in the online journal)

¹¹ The author to whom any correspondence should be addressed

1. Introduction

An international solar Ultraviolet (UV) filter radiometer comparison was held at the World Calibration Center for UV (WCCUV) of the Physikalisch-Meteorologisches Observatorium Davos, World Radiation Center (PMOD/WRC) from 25 May to 5 October 2017 [1].

The campaign was performed to assist UV monitoring stations of World Meteorological Organization/Global Atmosphere Watch (WMO/GAW) to link their solar UV radiation observations to the WMO/GAW reference scale through comparisons of the station instruments with the reference instruments operated by the WCCUV. The calibration of the WCCUV is supported by CMC's (Calibration and Measurement Capabilities) within the CIPM MRA¹².

The objective of the campaign was to provide a calibration traceable to the international system of units for all participating solar UV broadband filter radiometers, in view of homogenising solar UV irradiance measurements from all participating institutes.

The specific tasks of the campaign were to individually characterise each broadband filter radiometer with respect to the normalised spectral and angular responsivity in the laboratory following the standard operating procedures of the WCCUV. The calibration was obtained by direct comparison of solar irradiance measurements with the WCCUV reference spectroradiometers on the roof platform of PMOD/WRC.

This solar UV broadband filter radiometer comparison campaign followed three similar campaigns held in 1995 in Helsinki, Finland [2] with 20 participating radiometers, in 1999 in Thessaloniki, Greece [3] (21 radiometers) and in 2006 in Davos, Switzerland [4] (36 radiometers). 75 broadband radiometers from 37 Institutions participated in this latest comparison campaign. The radiometers were for the most part reference instruments within their respective regional or national networks.

In addition, to provide traceability of solar UV irradiance to the SI, an interlaboratory intercomparison (ILC) was organised between a subset of participants operating their own calibration facilities; 8 radiometers participated in this activity from the institutions ISO-CAL (USA), AEMET and INTA (Spain), LAP-AUTH (Greece), UIIMP (Austria), ARPA-Piemonte and ARPA-Valle d'Aosta (Italy) and BIRA-IASB (Belgium). The task of each participant to the ILC was to calibrate and characterise one of their radiometers at their own facility before and after the campaign at the WCCUV.

The measurement campaign at the WCCUV also allowed comparing the current calibration used by each participant with the calibration obtained from the campaign and to quantify the differences in solar UV measurements based on these calibrations. The campaign resulted in the release of calibration certificates to all participating institutes traceable

to the WCCUV reference and thus to the international system of units.

2. Methods

The calibration and intercomparison campaign took place at PMOD/WRC, Switzerland, from 25 May to 5 October 2017. The measurement platform is located on the roof of PMOD/WRC at 1610 m a.s.l., latitude 46.8° N, longitude 9.83° E. The measurement site is in the Swiss Alps and its horizon is limited by mountains to solar zenith angles (SZA) smaller than 75°; the Davos valley runs NE to SW.

The QASUME and QASUMELI [5] spectroradiometers were installed outdoors in April 2017. QASUMELI operated continuously until beginning of October, whereas QASUME missed the period from 22 May till 14 June 2017 due to external site audits.

The measurement data used for the calibration were obtained in the period 25 May to 5 October, totaling 134 measurement days. The measurement conditions in summer 2017 were very variable, with periods of clear sky, clouds, rain and snow.

The atmospheric total column ozone, TO_3 , was obtained from Brewer spectrophotometer #163 located next to QASUME. From 19 May till 30 June this Brewer participated in the 12th intercomparison campaign of the Regional Brewer Calibration Center Europe (RBCC-E) in Spain. Therefore, data from Brewer #072 was used. The total column ozone varied between 256 DU and 423 DU with a mean value of 304 DU over the measurement period.

75 filter radiometers from 58 Institutions of 37 countries took part in this campaign (see table 1). Their weighting functions for solar irradiance are: UVE (erythemal) [6], UVB (280 nm–315 nm), UVB320 (280 nm–320 nm), UVA (315 nm–400 nm) and UVG (280 nm–400 nm).

2.1. Calibration factor

The calibration measurements were carried out on the roof of PMOD/WRC. A detailed description of the method can be found in [7] and [8]. In the following the main steps of the procedure are summarized.

The calculation of the weighted irradiance from the radiometer data follows the equation published in [7] and [9]:

$$E_{UVE} = (U_{DET} - U_{offset}) \cdot C_D \cdot f(SZA, TO_3) \cdot Coscor, \quad (1)$$

where E_{UVE} is the erythemal weighted irradiance, U_{DET} and U_{offset} are the raw and dark signals from the radiometer respectively; C_D represents the calibration factor. The correction function, f , converts from the detector weighted solar irradiance to erythemal weighted irradiance (or other weighting function, see above). $Coscor$ corrects for the detector cosine error. The dark offset, U_{offset} , is determined every day during the night as the average over all measurements between 0 to

¹² PMOD/WRC follows the requirements for the competence of testing and calibration laboratories according to ISO/IEC 17025. PMOD/WRC is a designated institute of the Swiss Federal Office of Metrology, the Swiss signatory of the CIPM MRA (International Committee for Weights and Measures - Mutual Recognition Arrangement).

Table 1. Summary of participating radiometers to the UVC-II.

Number	Manufacturer	Type	Weighting
1	Kipp and Zonen (KZ)	CUV4	UVG
8	Kipp and Zonen	UV-S-AE-T / UV-S-AB-T	UVA+ UVE/UVB
3	Kipp and Zonen	UV-S-A-T	UVA
2	Kipp and Zonen	UV-S-B-T	UVB
11	Kipp and Zonen	UV-S-E-T	UVE
2	Sintec	UV-S-E-T	UVE
1	Sintec	UV-S-AE-T	UVA+UVE
3	Solar Light (SL)	SL501 (analog)	UVA
16	Solar Light	SL501 (analog)	UVE
9	Solar Light	SL501 (digital)	UVE
11	Yankee Environmental Systems, Inc. (YES)	UVB-1	UVE/UVB
2	Delta Ohm	LP UVI 02 AC/AV	UVE
1	Indium Sensor	1E.1-081	UVE
1	Genicom	GUVB-T12GD- 3LWH6	UVE
1	Eppley	TUVR	UVG
2	EKO	MS-212 W	UVE
1	Middleton Solar	UVR1-B2	UVB

4 UT and 20 to 24 UT. For radiometers with different weighting functions the same methodology is applied but the desired weighting function is used.

The calibration factor, C_D , is obtained by comparison with the solar spectrum measured by the spectroradiometer weighted with the spectral response function of the radiometer, E_d . Thus,

$$C_D = \frac{E_d}{U_{DET} - U_{offset}} \cdot \frac{1}{Coscor}. \quad (2)$$

To better compare correction functions, f , of different instruments, we define the normalized conversion function

$$f_n = \frac{f}{f(40 \text{ deg}, 300 \text{ DU})}. \quad (3)$$

We also define the erythemal calibration factor C as

$$C = C_D \cdot f(40 \text{ deg}, 300 \text{ DU}), \quad (4)$$

With these definitions, equation (1) can be written as:

$$E_{UVE} = (U_{DET} - U_{offset}) \cdot C \cdot f_n \cdot Coscor, \quad (5)$$

2.2. Instrument characterisation

The correction function, f , accounts for the mismatch of the detector spectral responsivity (SRF) and the chosen weighting function (e.g. UVE) and is calculated as

$$f(SZA, TO_3) = \frac{\int UVE(\lambda) E_{rad}(\lambda) d\lambda}{\int SRF(\lambda) E_{rad}(\lambda) d\lambda}, \quad (6)$$

where E_{rad} represents a set of solar spectra calculated with a radiative transfer model for different SZA and TO_3 . The SRF is obtained from laboratory measurement described in [7], and UVE represents the selected weighting function.

The angular response of UV radiometers usually deviates significantly from the nominal cosine response. The cosine correction function, $Coscor$, is used to correct the data. This correction depends on the atmospheric conditions and especially on the relative fraction of direct and diffuse radiation. For simplicity, the cosine correction that we applied to the data assumes an isotropic diffuse radiation distribution; the fraction of direct and diffuse radiation is modelled by a radiative transfer model in dependence of the solar zenith angle. For the determination of the calibration factor C_D only two cases were distinguished:

- Clear sky: A cosine correction function $1/f_{glo}$ in dependence on the SZA was used.
- Diffuse sky: Only the diffuse cosine correction factor $1/f_{dif}$ was applied to the calibration.

This simple approximation results in substantial uncertainties especially during rapidly changing scattered cloud conditions. Therefore, only the clear or completely overcast sky data were used for the calibration. Clear skies were manually selected using a sky camera. The following equations illustrate the derivation of $Coscor$:

$$f_{dir} = \frac{ARF(\Theta)}{\cos(\Theta)}, \quad (7)$$

$$f_{dif} = 2 \cdot \int_0^{\frac{\pi}{2}} ARF(\Theta) \sin(\Theta) d\Theta, \quad (8)$$

$$f_{glo} = f_{dir} \frac{E_{dir}}{E_{glo}} + f_{dif} \frac{E_{dif}}{E_{glo}}, \quad (9)$$

where f_{dir} is the cosine error of the radiometer, ARF represents the angular response function of the radiometer, f_{dif} the diffuse cosine error and f_{glo} the global cosine error of the radiometer. E_{dir} , E_{dif} and E_{glo} are the direct, diffuse and global irradiances respectively and are obtained from radiative transfer model calculations. For the data analysis of the UVC-II the model spectra were obtained using the sdisort solver of libRadtran 1.1 with the following input parameters: 16 streams, standard atmosphere midlatitude summer (afglms), albedo 0.035, AOD: $\alpha = 1.6$, $\beta = 0.01$, altitude = 0 m.a.s.l., pressure = 1013.25 mbar, SSA = 0.95, $g = 0.76$.

2.3. Uncertainty budget

The expanded uncertainty of the calibration factor C_D depends on the uncertainty of the following terms in equation (2):

- E_d is the detector weighted solar irradiance, recorded by the reference spectroradiometer [5].
- U_{DET} is the signal of the UV radiometer, averaged over the recording time of the spectroradiometer.

Table 2. Uncertainty budget for the calibration UV broadband radiometer; CMC’s of the WCCUV (* used for the WCCUV certificates until 01.08.2019 [5]). nui represents degrees of freedom used to calculate the standard uncertainty u.

Uncertainty component	Range	Unit	Type	Distribution	nui	u/%
E_d	1–10	UV-Index (UVI)	B	Normal	inf	1.1 (*2.3)
U_{DET}	0–1	V	B	Rectangular	inf	0.2
U_{offset}		V	B	Rectangular	inf	0.25
C_{var}	0.2	$Wm^{-2}nm^{-1}V^{-1}$	A	Normal	~3	0.6 (*1.5)
f_{var}			B	Rectangular	inf	0.6
d_{SRF}			B	Rectangular	inf	0.6
u(C)						1.55 (*2.9)
u(C)95						3.1 (*5.8)

- U_{offset} is the dark signal of the UV radiometer; calculated daily.

The uncertainty of the cosine correction (*Coscor*) does not add to the total uncertainty because it is included through the diurnal variability of the calibration factor C_{var} .

Additional uncertainty components arise from the calibration procedure,

- C_{var} is the variability of the calibration factor C_D during the calibration period.
- f_{var} accounts for the mismatch of the measured and modelled correction function, f_n .
- d_{SRF} : The uncertainty of the SRF measurement is composed of the extrapolation to 400 nm as well as the measurement uncertainty of the SRF itself.

The nominal uncertainty budget is summarized in table 2. The expanded uncertainties stated on the individual certificates issued for the campaign are calculated from the actual data of the specific radiometer calibration and these deviate slightly from the values shown in table 2.

3. Results

The two reference spectroradiometers QASUME and QASUMEII measured synchronised solar irradiance spectra in the range 290 nm to 400 nm every 0.25 nm every 15 to 30 minutes. The comparison of the solar irradiance spectra followed the standard operating procedure of a QASUME intercomparison, i.e. the spectra recorded by the two reference spectroradiometers were convolved to a 1 nm slit width and wavelength adjusted to a common wavelength scale using the matSHIC algorithm [10]. The comparison of all measurements at selected wavelengths and the average over the measurement period is shown in figure 1.

As can be seen in figure 1 the average ratio of 1.0 and a standard deviation of less than 3% between the two instruments are well within the combined expanded uncertainties of $\pm 3.7\%$ [5].

The QASUMEII data was used as reference for the calibration of the broadband radiometers. The spectroradiometer was calibrated several times during the comparison period using a portable monitor system with 250 W lamps (T61251, T68522,

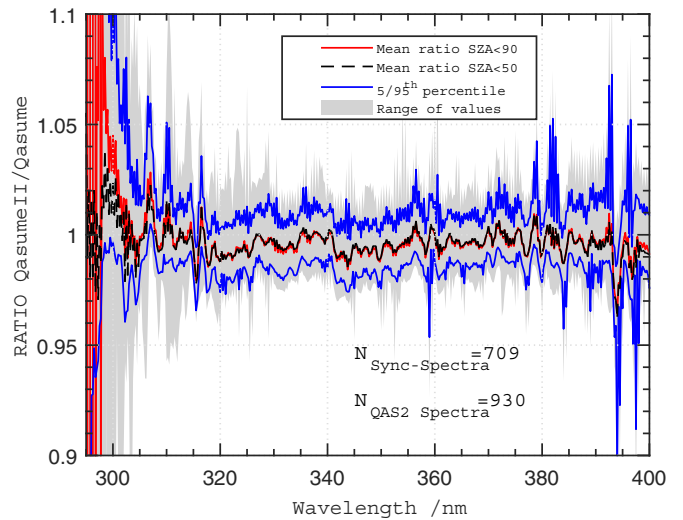


Figure 1. Mean ratio of QASUMEII / QASUME (clear sky data) at PMOD/WRC, 8 April 2017 to 8 October 2017.

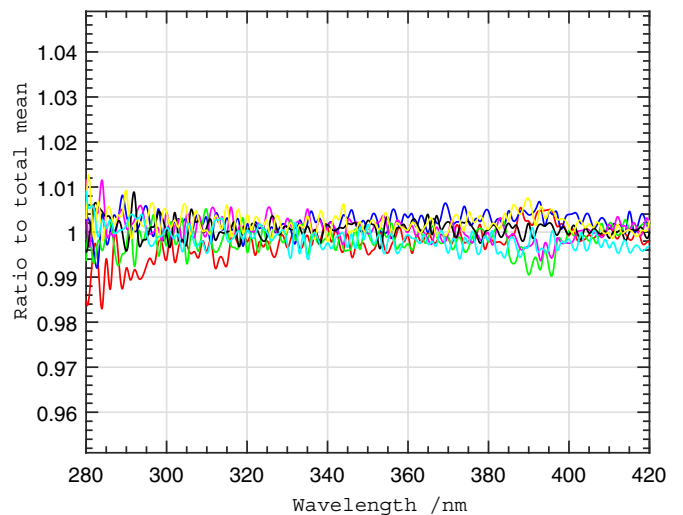


Figure 2. QASUMEII spectral responsivity ratio to the average. The calibrations were based on transfer standard T68523, Day of Year (DOY) 166 till 247, 2017.

T68523 and KS020). The spectroradiometer remained stable to within $\pm 1\%$ in the period (figure 2).

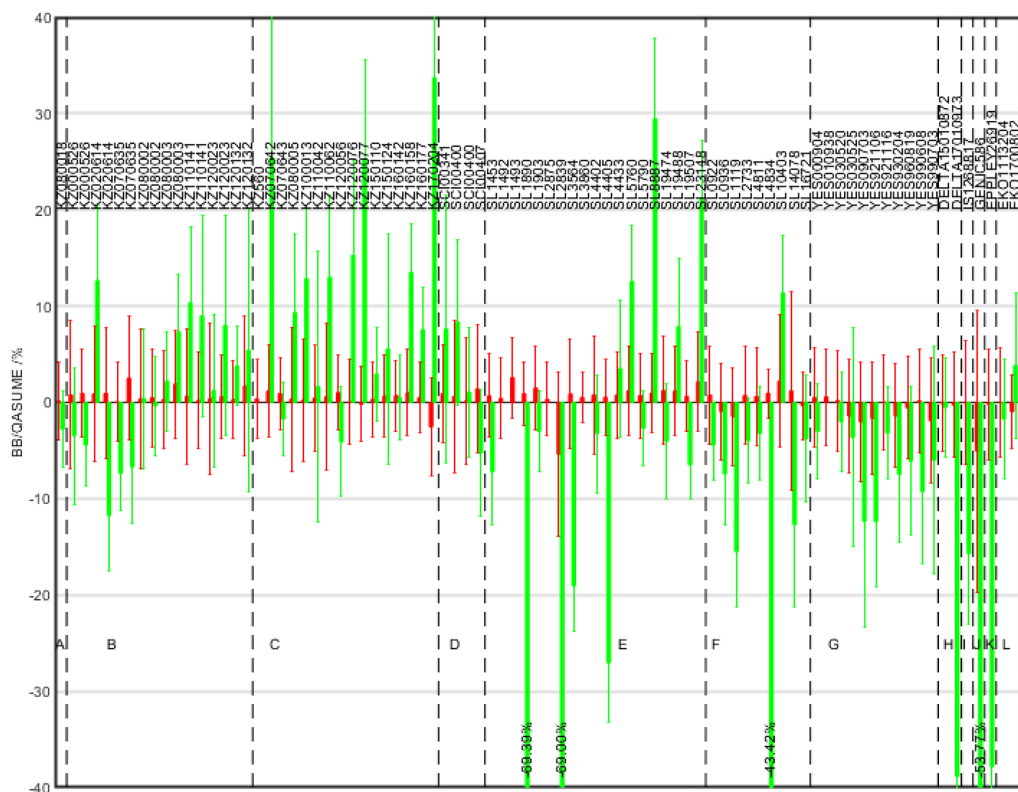


Figure 3. Comparison of the original (USER, green) and the new WCCUV-calibration (PMOD, red) for all participating radiometers. The whiskers show the variability during the intercomparison for each radiometer. A: KZ-CUV4, B: KZ-AE/AB, C: KZ-A/E/B, D: Scintec, E: SL501 (analog), F: SL501 (digital), G: YES UVB-1, H: Delta Ohm, I: Indium Sensor, J: Genicom, K: Eppley, L: EKO, M: Middleton Solar

3.1. The campaign

The raw data of the broadband UV radiometers of the whole campaign (all sky conditions, without precipitation) were converted to weighted solar irradiance using the campaign derived WCCUV-calibration factors (PMOD) on the one hand, and the USER supplied original calibration factors on the other. The PMOD dataset was calculated using equation (5) and auxiliary measurements from a direct UV radiometer to differentiate between clear sky and diffuse sky.

The summary results of the UVC-II is shown in figure 3. Applying the WCCUV-calibration to the broadband dataset results in UVI values which deviate to the QASUMEII reference to within $\pm 5\%$ for 73 out of 75 instruments (97%). 32 (43%) of the datasets derived using the USER calibration factors are within $\pm 5\%$, 48 (64%) are within $\pm 10\%$ and 27 (35%) exceed $\pm 10\%$. Two datasets deviate even by nearly 70% from the measurements of the reference spectroradiometer. Table 3 summarizes the statistics of the comparison shown in figure 3. In table 3, the 75 radiometers are separated into 3 subgroups. Although the mean deviation from the reference is low for all three datasets the variability is very high for those radiometers calibrated using just the calibration factor C alone. Figure 4 is an example of this group showing the relative ratio between the two data sets for one radiometer with respect to the reference measurements obtained from QASUMEII. Adding the correction function, f (but no $Coscor$), improves the result significantly. The

Table 3. Statistics of the USER-calibration quality for the instruments of the UVC-II listed according to their latest calibration procedure (outliers with deviations greater than 40% were excluded): Complete usage of equation (1) (FULL), use of the correction function (f_n) and use of a single calibration factor (C).

Procedure	# Devices	Mean Bias /%	Percentile /%	
			5	95
FULL	22	-2.3	-13.8	6.1
f_n	9	-1.2	-11.1	12.9
C	44	+1.7	-30.3	26.6

USER-calibrations using all correction factors of equation (1) obtain data with a bias between -14% and $+6\%$.

For data used for public health information such as the UV-Index, the error in absolute units is an alternative quality criterion to the relative ratio shown in figure 3. The analysis of the median difference of the 55 UVE-weighted radiometers to the reference dataset with USER-calibration show that the derived UV-Index is within ± 0.61 UVI. Only 6 datasets have biases of more than ± 1 UVI, 2 are below -1.5 UVI.

3.1.1. Effect of the spectral response mismatch. The SRF of each radiometer was measured during the UVC-II. Although they are similar for a specific radiometer type they deviate substantially from each other, as shown in figure 5 for Kipp and Zonen (KZ) UV-S-E-T, Solar Light (SL)

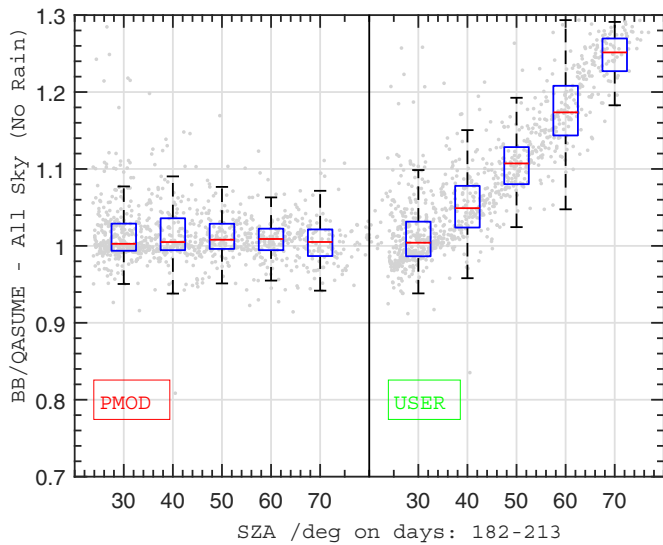


Figure 4. Erythemal weighted broadband irradiance vs. QASUMEII reference data - plotted against the solar zenith angle. Left: WCCUV-calibration (PMOD); right: USER-calibration based on a single calibration factor only. In this example the data of UVE channel of the Kipp and Zonen, SN. 120023, was used. On each box, the central mark indicates the median, and the bottom and top edges of the box indicate the 25th and 75th percentiles, respectively. The whiskers extend to the most extreme data points not considering outliers. Outliers are defined as data points outside the 99.3% confidence interval, assuming a normal probability distribution [11].

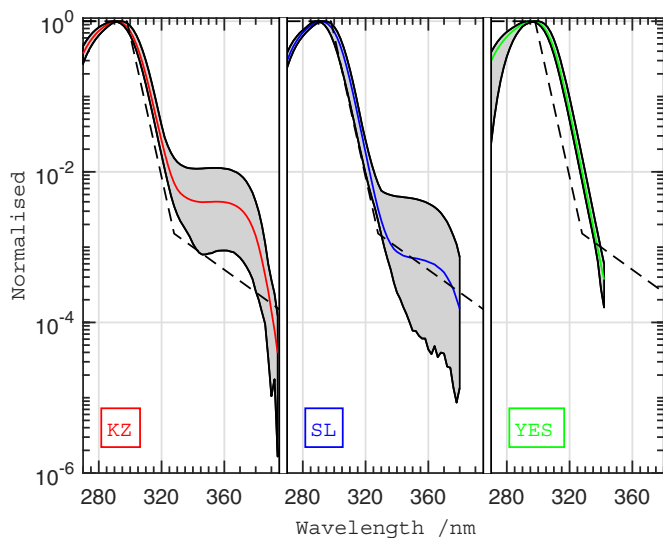


Figure 5. The variability of the spectral responsivities of KZ, SL and YES radiometers. The colored lines show the mean, the black lines the 5th and 95th percentiles, the black dashed lines the erythema weighting function [6].

501 and Yankee Environmental Systems, Inc. (YES) UVB1 radiometers, representing the three main types of radiometers participating in the campaign. An individual correction function, f_n , was derived using equation (3). Neglecting this correction function leads to a large uncertainty in the derived erythemally weighted irradiance. The magnitude of the correction can be obtained from the two-dimensional

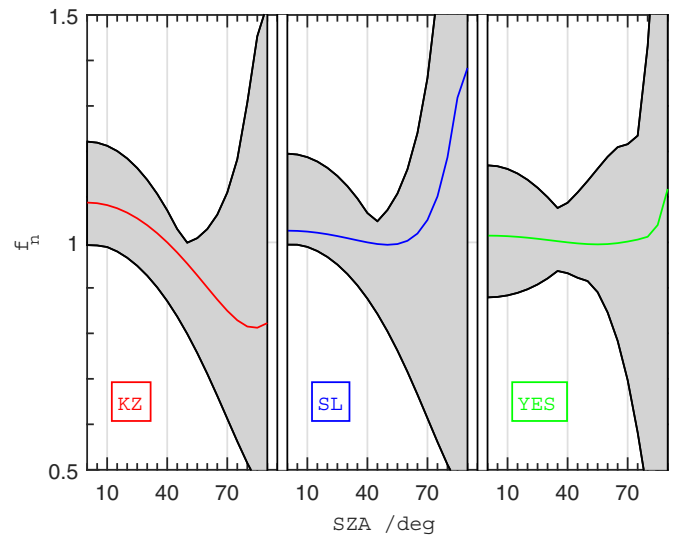


Figure 6. Mean of the correction function f_n for a fixed ozone value of 300 DU for the participating KZ (left), SL (middle) and YES (right) radiometers. The shaded area shows the range of values of the correction function for ozone ranging from 260 DU till 400 DU.

correction function f_n . Figure 6 shows the mean of KZ, SL and YES correction functions of the UVC-II for ozone values ranging from 260 DU to 400 DU. Both, the mean at 300 DU and the range of values for all ozone values and SZA are a measure of the uncertainty introduced by omitting this correction. The mean correction shows a strong dependence on the solar zenith angle for the KZ and a small dependence for SL and YES radiometers for $SZA < 75^\circ$. The mean correction at 300 DU is smaller than 1.5% for $SZA < 75^\circ$, but the range of values exceeds $\pm 20\%$ for all radiometer types—even for low solar zenith angles. It should be noted that a small uncertainty (less than 1%) is introduced by the extrapolation of the measured SRF to 400 nm, which is especially the case for YES UVB-1 radiometers (see [12]).

3.1.2. Effect of the angular response mismatch. In analogy to the section before, figure 7 shows the cosine correction for the same set of radiometers. The set of KZ radiometers have small cosine correction functions and the homogeneity is very high. For SL radiometers, both, the correction as well as the variability within the group is high. The cosine correction is largest for YES radiometers with a small variability within this set. The maximal correction is 4% for the KZ, 18% for the SL and 27% for the YES radiometers. Therefore, a cosine correction is essential for SL and YES radiometers. Without cosine correction a YES radiometer underestimates the actual erythemal irradiance significantly. For SL an individual correction function should be obtained whereas for YES and the KZ radiometers one could consider taking a mean cosine correction function for a set of similar radiometers belonging to the same network.

It should be noted that choosing the correct cosine correction function (clear sky vs. diffuse sky) is essential to obtain low uncertainties during the calibration period (see

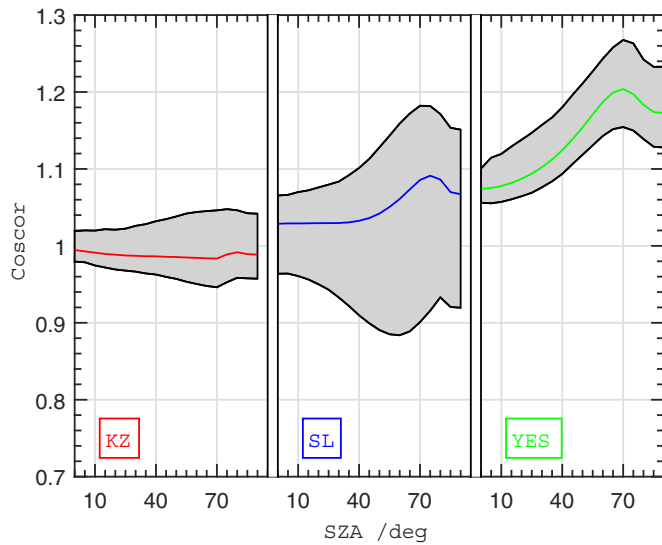


Figure 7. Mean of the cosine correction of the radiometers participating at the UVC-II for a KZ (left), SL (middle) and YES (right) radiometer. The shaded area shows the range of the correction function for the three radiometer types.

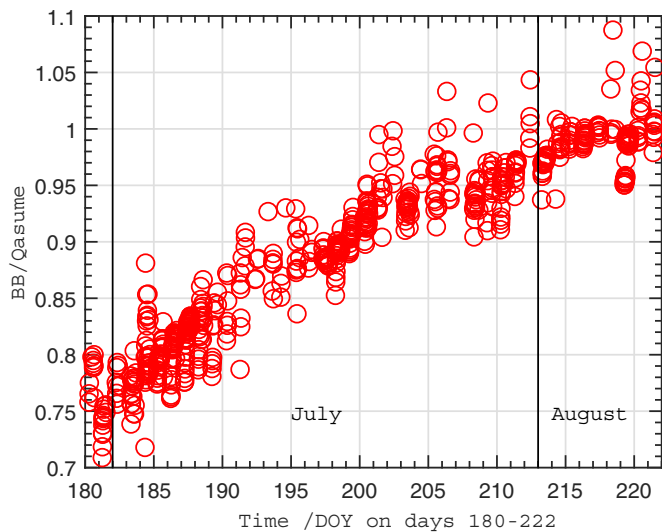


Figure 8. The ratio of the SL2839 irradiance data relative to the reference reveals the sensitivity change after the renewal of the desiccant on 29 June 2017.

section 2.3, factor C_d). The best method is manual selection of the clear sky periods using for example sky images. For routine data recording all year round, one can use an averaged $Coscor(SZA)$, independent on the atmospheric conditions (see e.g. [13]), or it becomes a non-trivial task using auxiliary data, e.g. [14] or [15].

3.1.3. Humidity. Humidity is the environmental factor which affects mostly the sensitivity of current UV broadband filter radiometers through the susceptibility of the filters used to produce the desired spectral response function [16]. SL2839 can act as a good example to illustrate the change in the response of an instrument from high to low humidity, i.e. the

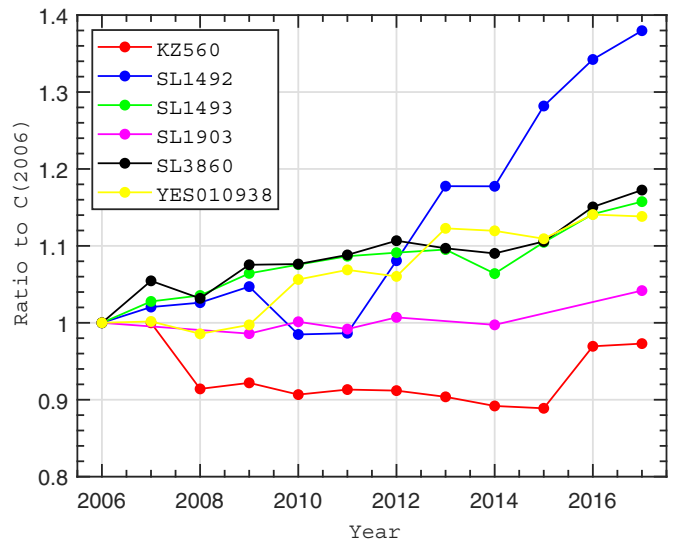


Figure 9. Calibration factor changes of 6 selected broadband filter radiometers.

Table 4. Statistics of the USER-calibration quality for the instruments of the UVC-II listed according to their latest calibration date (outliers with deviations greater than 40% were excluded). The last line shows the statistic of the WCCUV-calibration.

Year	Number of Devices	Mean Bias /%	Percentile /%	
			5	95
2006	14	-2.2	-11.3	9.6
2012–2015	13	+0.6	-14.4	22.2
≥ 2015	40	+1.2	-13.9	24.9
≥ 1987	75	+0.1	-17.5	23.4
2017 (WCCUV)	75	+0.3	-1.9	2.0

Table 5. Institutes participating to the Interlaboratory comparison (*accredited institutes following the ISO/IEC 17025 norm).

Institute	Instrument	Country
ARPA Aosta	KZ000526 (UVA, UVE)	Italy
ARPA Piemonte*	KZ080003 (UVA, UVE)	Italy
ISOcal*	KZ110141 (UVA, UVB)	USA
UIIMP Innsbruck	SL19507	Austria
AEMET Madrid	YES030520	Spain
LAP-AUTH	YES921116	Greece
INTA	YES990608	Spain
BIRA-IASB	EKO111320-4	Belgium

renewal of the desiccant at the beginning of the period (see figure 8). Within a timescale of 20 days the calibration factor changed by 20%.

3.1.4. Sensitivity drift of radiometers. The calibration frequency of a broadband filter radiometer is an essential element in assessing the uncertainty of its solar UV measurements. Only by knowing the instrument calibration before and after a measurement period can the data be quality assessed and produce traceable solar UV irradiance data. From the history of past calibrations, one can estimate typical degradation timescales of radiometers measuring solar UV irradiance.

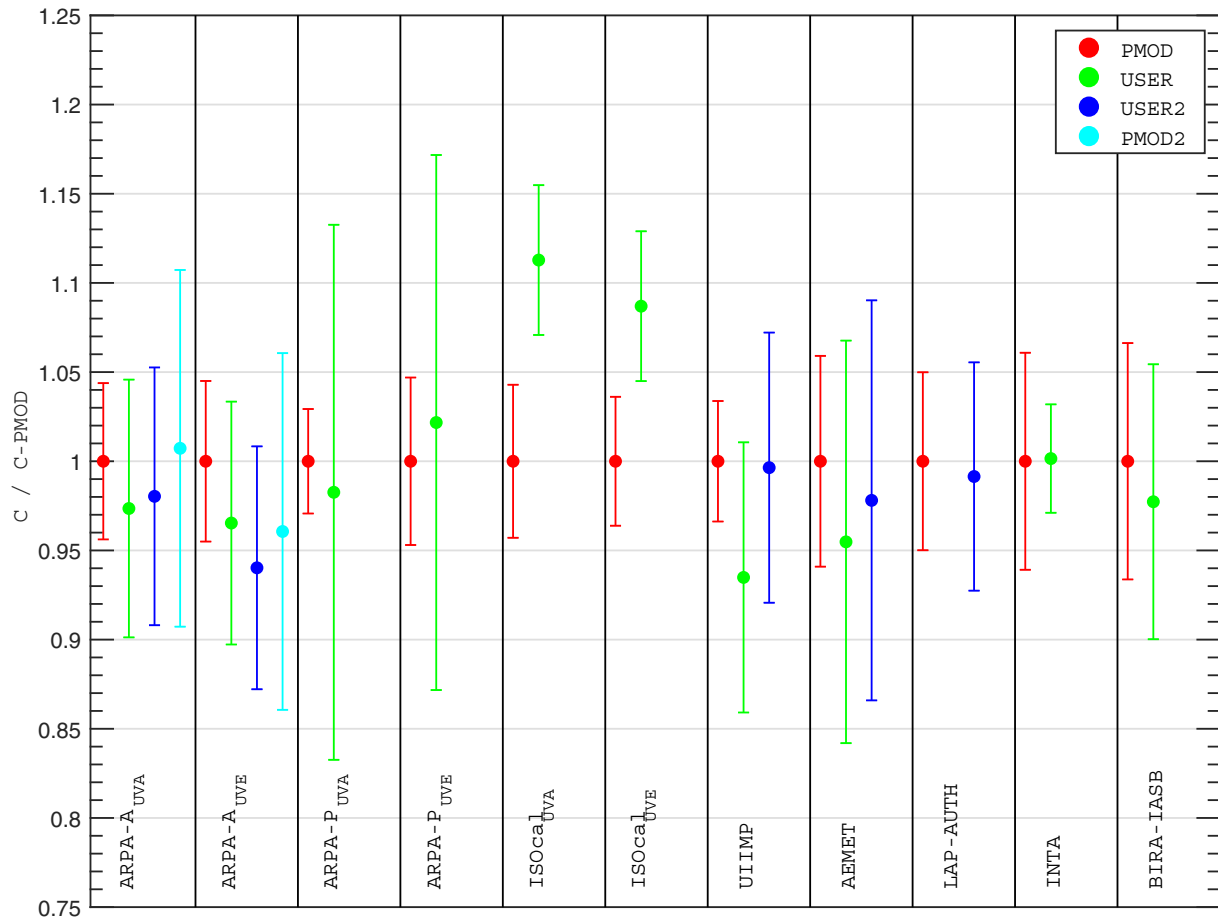


Figure 10. Comparison of the operational calibration by the participant (USER) and the calibration obtained in the UVC-II campaign (PMOD). Data shown in blue indicate calibration factors derived after the return of the devices to their home institutes (USER2 and PMOD2).

The following radiometers—most belong to the WCCUV—have been calibrated annually since 2006: SL1492, SL1493, SL1903, SL3860, KZ560, YES010938. Figure 9 shows that the calibration factors increase by 1.5% to 3.5% per year for the Solar Light radiometers, which means that the responsivity decreases by the same rate. This results in a calibration frequency of at least once every three years to achieve an uncertainty less than 10%. The KZ560 shows unpredictable sensitivity changes in the order of 10% between subsequent calibrations. This is probably due to high intake of humidity of the radiometer. In contrast, SL1903 shows only a very small variability of its sensitivity. The reason is very likely the custom-made sealing of the instrument and annual nitrogen purging procedure (Laurent Vuilleumier, personal communication).

[17] recommend an annual recalibration because of well-known sensitivity changes of UV radiometers. The average of the last calibration year for the 75 radiometers is 2012. The oldest calibration is three decades old. Table 4 summarizes the statistics of the calibration results relative to the date of the last USER-calibration. The group of well-maintained radiometers already participating in the 2006 campaign [4] show a low offset and variability against the reference. The table does not show any significant dependence on the calibration age because of the high variability within each group caused by

the differences in the USER-calibration procedures (see section 3.1, table 3).

4. Interlaboratory comparison

Seven of the eight UV broadband filter radiometers participating in the UVC-II were calibrated and characterised at their home facilities before being sent to the WCCUV, following a similar procedure as described in [12] and one radiometer was calibrated after being returned to the home institute after the campaign. These radiometers are from 6 Countries, of which 5 are from Europe. The 4 different radiometer types are Kipp and Zonen (3), YES UVB-1 (2), analog Solar Light V. 501 (1), and one EKO MS 212 W. The filter weighting functions are approximating the erythemal action spectrum (UVE) or UVB. Three devices are dual channel radiometers (UVA and UVE/UVB). Table 5 provides an overview of the radiometers and their home institutes.

Figure 10 shows a summary of the results of the interlaboratory comparison, showing the calibration factors with their estimated expanded relative uncertainties ($k = 2$) as derived from the home institutes relative to the factors resulting from the WCCUV calibration. For the YES990608, the USER expanded uncertainty corresponds to the measurement

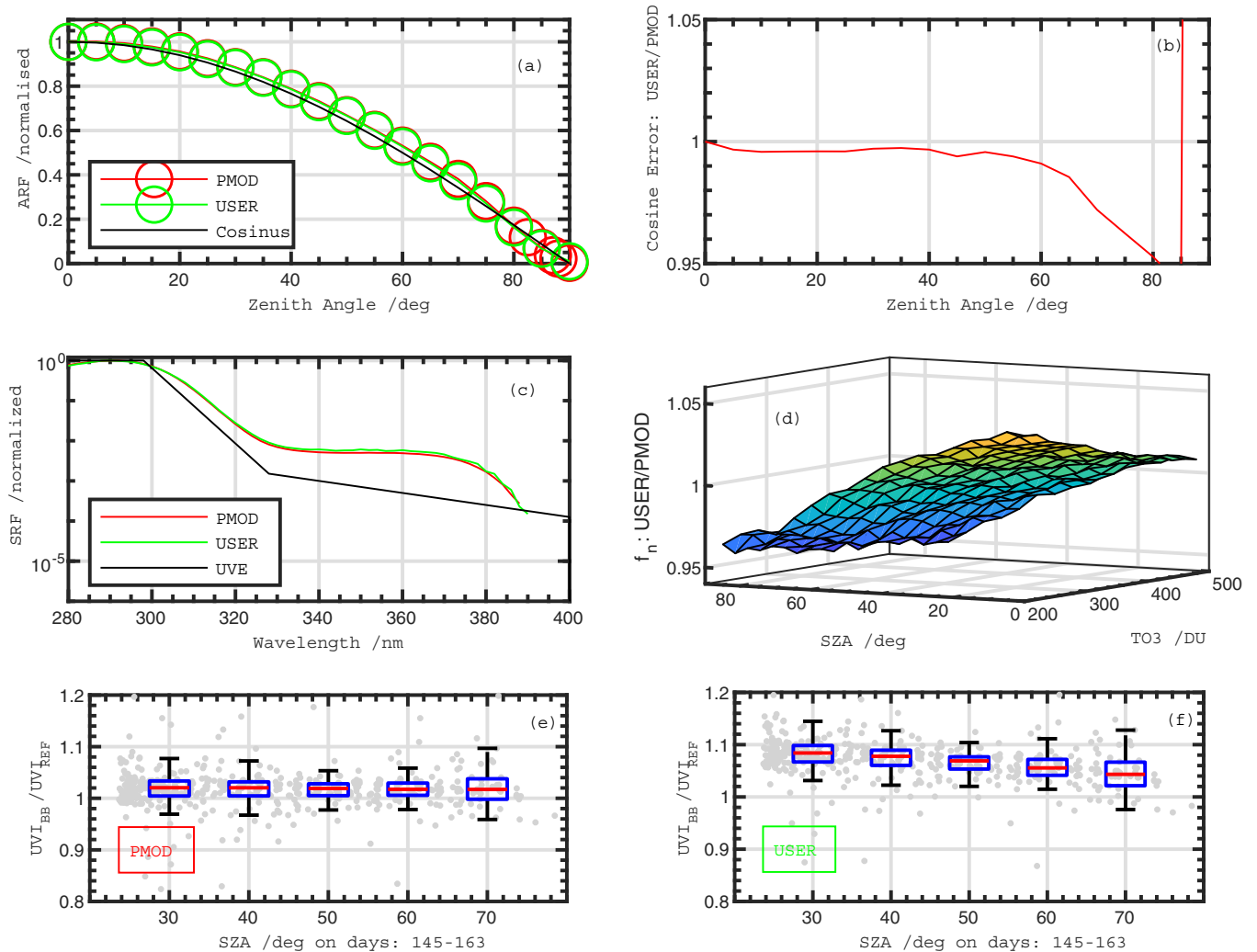


Figure 11. Response functions ARF (a) and SRF (c), the ratio between the USER to PMOD cosine errors (b) and the ratio of the USER and PMOD correction functions f_n (d) of KZ080003. Panels (e) and (f) show the UVI data relative to the reference using the PMOD (e) and USER (f) calibration. On each box, the central mark indicates the median, and the bottom and top edges of the box indicate the 25th and 75th percentiles, respectively. The whiskers extend to the most extreme data points not considering outliers. Outliers are defined as data points outside the 99.3% confidence interval, assuming a normal probability distribution [11].

uncertainty only ($k = 2$) and does not include further uncertainty contributions as discussed in section 2.3. For most of the participating institutes, the calibrations were within the combined expanded uncertainties, with only KZ110141 from ISOcal showing a larger difference to the WCCUV calibration.

Detailed results can be found in the annex of the UVC-II report [1]. As an example, figures 11(a)–(d) shows the results of the laboratory characterisation of KZ080003 for its UVE channel. The measurements of the angular (a) and spectral responsivity (c) are in very good agreement. The corresponding cosine errors deviate by less than 1% for zenith angles smaller than 60° (b). The correction function, f_n , calculated from the SRFs, differ by less than $\pm 4\%$ as a function of the SZA (d).

Figures 11(e) and 11(f) shows the UVI produced using the WCCUV-calibration (e) and the USER calibration (f) relative to the reference dataset using all quality assured data from the campaign. The difference of the calibration factor, C , leads to the systematic offset of the UVI using the USER calibration. Because this institute did not use a cosine correction function,

the difference of the correction functions shown in figure 11(d) dominates the result of the UVI comparison (figure 11(f)) with high ratios at noon and lower ratios at sunset and sunrise.

4.1. Instrument stability

In contrast to the agreed ILC protocol, not all institutes could characterise and calibrate the radiometer on its return to the home institute after the UVC-II campaign: For ARPA Piemonte, INTA and BIRA-IASB the instrument arrived after the calibration period (late autumn); as mentioned previously, LAP-AUTH calibrated the instrument only after the return (no initial calibration); KZ110141 from ISOcal suffered from an electrical shock during the post calibration. Only ARPA Aosta, UIIMP Innsbruck and AEMET Madrid were able to perform the post calibration (USER2). In addition, a QASUME site audit at ARPA Aosta was performed in September 2017 by the WCCUV. Through this site visit a PMOD2 calibration of KZ000526 was derived at its home site. The USER2 and PMOD2 results are added to figure 10 and

show that the sensitivity of the UVA channel of KZ00526 decreased by 0.7% (PMOD2: 0.8%) while the sensitivity of the UVE channel increased by 2.6% (PMOD2: 3.9%); the sensitivity of YES030520 increased by +3.6% between the two AEMET calibrations performed in June 2016 and October 2017, whereas the responsivity of SL19507 decreased by 6% between the initial calibration in June and the recalibration in October. The calibration factors of SL19507 in 2018 and 2019 show also a large variability of more than 5%, indicating that this radiometer is less stable than others.

5. Conclusion

The 2nd UV calibration campaign at the WCCUV has been described. With 75 participating reference instruments from all over the world it was the largest campaign for UV broadband filter radiometers ever performed. All radiometers were characterised in the laboratory of the WCCUV and calibrated outdoors relative to the QASUME-II reference spectroradiometer. During the three-month calibration period all radiometers were returned to the home institutes accompanied by a certificate providing traceability to the international system of units. The calibration uncertainty was less than 6% for the majority of the radiometers.

The deviation to the original calibration factors was analysed. From this data one can extract three components affecting the overall measurement uncertainty of solar UV irradiance measurements using UV broadband filter radiometers on different time scales:

- Short term (diurnal): Usage of the correction functions f_n and $Coscor$.
- Mid term (months): Control of the humidity inside the radiometer.
- Long term (years): Recalibration interval.

In addition, most factory calibrations of UV radiometers are delivered without any statement of the calibration uncertainty.

Within the campaign, a subset of eight instruments participated in an interlaboratory comparison. A comparison of the calibration factors showed that the USER and the WCCUV calibrations agree within the expanded uncertainties for 9 out of 11 calibrations. The sensitivity of three instruments was checked after the return to their home institutes. A notable change in the sensitivity was observed only for one device.

Following the standard practice implemented at the World Radiation Centre for Pyrheliometer and Pyrgeometer comparisons, the next UV calibration campaign UVC-III is planned for 2022, 5 years after the UVC-II. The outcome of the ILC could be improved by a predefined protocol, signed and agreed on by all the participating laboratories following the guideline of the Consultative Committee for Photometry and Radiometry (CCPR) for ILCs.

Acknowledgments

We would like to acknowledge the active support of the PMOD/WRC staff in the preparation and organisation of the intercomparison campaign. The instrument owners provided

the calibrated data for the intercomparison period using their home calibration. Special thanks to Christian Thomann for the help in installing the radiometers and the repair of various KZ radiometers, our electronic civil servants for repairing the broken Solar Light radiometers, the staff of our administrative department for organising the shipping of the instruments and Luca Egli for his support in maintaining the reference spectroradiometers. We thank Laurent Vuilleumier for providing the history data of SL1903, José María San Atanasio and Irene Melero for the calibration of the radiometer from AEMET, Nuno Pereira for the calibration of the BIRA-IASB radiometer, Chrysanthi Topaloglou for the characterisation of the radiometer from LAP-AUTH.

ORCID iD

Alkis Bais  <https://orcid.org/0000-0003-3899-2001>

References

- [1] Hülsen G and Gröbner J 2018 *Report of the Second Int. UV Filter Radiometer Calibration Campaign UVC-II* (Geneva: WMO/GAW No. 240 World Meteorological Organization)
- [2] Leszczynski K, Jokela K, Ylianttila L, Visuri R and Blumthaler M 1998 *Photochem. Photobiol.* **67** 212–21
- [3] Bais A F, Topaloglou C, Kazadzis S, Blumthaler M, Schreder J, Schmalwieser A, Henriques D and Janouch M 1999 *Report of the LAP/COST/WMO Intercomparison of Erythemal radiometers, Thessaloniki, Greece, 1999* (Geneva: WMO/GAW No. 141 World Meteorological Organization Geneva)
- [4] Gröbner J, Hülsen G, Vuilleumier G L, Blumthaler M, Vilaplana J M, Walker D and Gil E 2007 *Report of the PMOD/WRC-COST Calibration and Intercomparison of Erythemal Radiometers* (Luxembourg: Office for Official Publications for the European Communities)
- [5] Hülsen G, Gröbner J, Nevas S, Sperfeld P, Egli L, Porrovecchio G and Smid M 2016 *Appl. Opt.* **55** 7265–75
- [6] Webb A, Slaper H, Koepke P and Schmalwieser A 2011 *Photochem. Photobiol.* **87** 483–6
- [7] Hülsen G and Gröbner J 2007 *Appl. Opt.* **46** 5877–86
- [8] Seckmeyer G, Bais A F, Bernhard G, Blumthaler M, Booth C R, Lantz R, McKenzie R, Disterhoft P and Webb A 2007 *Instruments to Measure Solar Ultraviolet Radiation. Part 2: Broadband Instruments Measuring Erythemally Weighted Solar Irradiance* (Geneva: WMO/GAW No. 164 World Meteorological Organization)
- [9] Gröbner J et al 2005 *Appl. Opt.* **44** 5321–31
- [10] Slaper H, Reinen H A J M, Blumthaler M, Huber M and Kuik F 1995 *Geophys. Res. Lett.* **22** 2721–4
- [11] MathWorks 2020 ‘Documentation, Box Plot’ (<https://ch.mathworks.com/help/stats/boxplot.html>)
- [12] Hülsen G et al 2008 *Atmos. Chem. Phys.* **8** 4865–75
- [13] Blumthaler M 2004 *Radiat. Prot. Dosim.* **111** 359–62
- [14] Lakkala K et al 2018 *Atmos. Meas. Tech.* **11** 5167–80
- [15] Landelius T and Josefsson W 2000 *J. Geophys. Res. A* **105** 4795–802
- [16] Huber M, Blumthaler M, Schreder J, Bais A and Topaloglou C 2002 *Appl. Opt.* **41** 4273–7
- [17] Webb A, Gröbner J and Blumthaler M 2006 *A Practical Guide to Operating Broadband Instruments Measuring Erythemally Weighted Irradiance EUR 22595* (Luxembourg: Office for Official Publications for the European Communities)